

# Self-similarity relations for cooling superfluid neutron stars

P. S. Shternin<sup>1,2\*</sup>, D. G. Yakovlev<sup>1</sup>

<sup>1</sup>*Ioffe Institute, Politehnicheskaya 26, 194021 St. Petersburg, Russia*

<sup>2</sup>*St. Petersburg Polytechnic University, Politehnicheskaya 29, 195251, St. Petersburg, Russia*

Accepted . Received ; in original form

## ABSTRACT

We consider models of cooling neutron stars with nucleon cores which possess moderately strong triplet-state superfluidity of neutrons. When the internal temperature drops below the maximum of the critical temperature over the core,  $T_C$ , this superfluidity sets in. It produces a neutrino outburst due to Cooper pairing of neutrons which greatly accelerates the cooling. We show that the cooling of the star with internal temperature  $T$  within  $0.6 T_C \lesssim T \leq T_C$  is described by analytic self-similar relations. A measurement of the effective surface temperature of the star and its decline, supplemented by assumptions on star's mass, radius and composition of heat-blanketing envelope, allows one to construct a family of cooling models parametrized by the value of  $T_C$ . Each model reconstructs cooling history of the star including its neutrino emission level before neutron superfluidity onset and the intensity of Cooper pairing neutrinos. The results are applied to interpret the observations of the neutron star in the Cassiopeia A supernova remnant.

**Key words:** dense matter – equation of state – neutrinos – stars: neutron – supernovae: individual (Cassiopeia A) – X-rays: stars

## 1 INTRODUCTION

It is well known that observations of cooling neutron stars allow one to explore still uncertain properties of superdense matter in neutron star interiors (e.g., Yakovlev & Pethick 2004). Here, we consider cooling of neutron stars with nucleon cores. We assume that a star is not too young (with the age  $t \gtrsim 10 - 200$  yr) so that it is thermally relaxed (isothermal) inside except for the thin heat-blanketing layer near the surface. In addition, we assume that the star is on the neutrino cooling stage ( $t \lesssim 10^5 - 10^6$  yr) meaning that it cools from inside via neutrino emission from its interior (mainly from the core). The thermal photon surface luminosity is much lower than the neutrino luminosity and adjusts itself to the current internal thermal state. In this way, the thermal emission from the surface reflects the intensity of the neutrino emission that depends on the properties of superdense matter in neutron star core.

There are two basic phenomena that can be tested by neutron star cooling: (i) the operation of powerful direct Urca process of neutrino emission in inner cores of massive neutron stars; (ii) the presence of nucleon superfluidity in neutron star cores. The direct Urca process is regulated by the symmetry energy of neutron star matter (becomes allowed at sufficiently large symmetry energy which results in rather large fraction of protons). To simplify our analysis, we assume that the direct Urca process is not allowed and focus on the effects of superfluidity. This is equivalent of using the minimal cooling theory (Page et al. 2004; Gusakov et al. 2004).

Following the standard minimal cooling theory we consider

two superfluids in the neutron star core – singlet-state pairing of protons and triplet-state pairing of neutrons. The appropriate critical temperatures depend on the density  $\rho$  and will be denoted as  $T_{cp}(\rho)$  and  $T_{cn}(\rho)$ , respectively. Unfortunately, nucleon superfluidity is a very model dependent phenomenon. Typically, the  $T_{cp}(\rho)$  and  $T_{cn}(\rho)$  profiles over the stellar core have bell-like shapes (e.g., Lombardo & Schulze 2001). Various models predict very different profiles, so that it is instructive to consider these profiles as unknowns and try to constrain them from observations of cooling neutron stars. As widely discussed in the literature, the effects of proton and neutron superfluidities on neutron star cooling are different (e.g., Page et al. 2009). Proton superfluidity mainly suppresses neutrino emission processes involving protons. As for neutron superfluidity, it also suppresses the traditional processes of neutrino emission, but its onset may initiate a powerful neutrino outburst due to Cooper pairing of neutrons. Neutron superfluidity occurs when the temperature  $T$  in the cooling star falls down to the maximum critical temperature of neutrons in the core,

$$T_C = \max\{T_{cn}(\rho)\}, \quad (1)$$

and can strongly accelerate the cooling. This effect has been used by Page et al. (2011) and Shternin et al. (2011) to interpret the results by Ho & Heinke (2009) and Heinke & Ho (2010) who analysed the observations of the neutron star in the Cassiopeia A (Cas A) supernova remnant.

Following Page et al. (2011) and Shternin et al. (2011), we consider the cooling scenario in which proton superfluidity is much stronger than neutron one. Then, proton superfluidity appears at the early cooling stage and suppresses neutrino emission processes in-

\* E-mail: pshternin@gmail.com

volving protons and proton heat capacity. Subsequent cooling history contains two stages, prior ( $T \geq T_C$ ) and after ( $T < T_C$ ) the onset of neutron superfluidity. The first stage represents a slow cooling of the star. Such a cooling is described by simple analytic relations which allow one to perform model-independent analysis of the slow neutrino cooling rate (Yakovlev et al. 2011). Here, we focus on the second stage,  $T < T_C$ , and show that as long as  $T \gtrsim 0.6T_C$  neutron star cooling is described by self-similar analytic equations which can be used to reconstruct the cooling history of the star from observational data.

## 2 COOLING EQUATIONS

We follow the cooling theory of neutron stars with isothermal interiors at the neutrino cooling stage (e.g., Yakovlev et al. 2011). The basic cooling equation (including the effects of General Relativity) is

$$\frac{dT}{dt} = -\ell(T) = -\frac{L_\nu(T)}{C(T)}. \quad (2)$$

Here,  $T$  is the redshifted internal temperature,  $t$  is Schwarzschild time,  $\ell(T)$  is the neutrino cooling rate,  $L_\nu(T)$  is the neutrino luminosity and  $C(T)$  is the integrated heat capacity of the star. It is the redshifted temperature  $T$  which is constant over the isothermal internal region of the star;  $L_\nu(T)$  and  $C(T)$  in equation (2) also have to be redshifted. If  $\ell(T)$  is known, one can immediately write down a formal solution of the cooling problem

$$t - t_i = \int_{T_i}^T \frac{dT'}{\ell(T')}, \quad (3)$$

where  $T_i$  is the temperature at some initial moment of time  $t = t_i$ . This expression describes the evolution of the internal temperature  $T(t)$ . The surface temperature of the star,  $T_s(t)$ , can be calculated then from the internal one using the relation between the internal and surface temperatures (e.g., Potekhin, Chabrier & Yakovlev 1997).

Let  $t = t_C$  refer to the onset of neutron superfluidity in the neutron star core (at  $T = T_C$ , where  $T_C$  has to be treated as the maximum value of the redshifted critical temperature for neutron superfluidity in the stellar core). Before the onset, we have a slow cooling with  $L_\nu(T) \propto T^8$ ,  $C(T) \propto T$  and  $\ell(T) \propto T^7$ . In our notations, this slow cooling is described by

$$t = \frac{t_C}{\tau^6}, \quad \text{at } \tau \equiv \frac{T}{T_C} \geq 1 \quad \text{that is } t \leq t_C. \quad (4)$$

Note that in this case

$$\ell(T) = \frac{T}{6t}. \quad (5)$$

This solution is obtained with the standard initial condition widely used in the neutron star cooling problem:  $T_i \rightarrow \infty$  as  $t_i \rightarrow 0$ . Here and below, we consider the cooling solutions  $t = t(\tau)$  as functions of the dimensionless quantity  $\tau$ .

After the neutron superfluidity onset, from equation (3) we have

$$t = t_C + \int_{T_C}^T \frac{dT'}{\ell(T')} \quad \text{at } t > t_C. \quad (6)$$

At this stage, we need the neutrino cooling rate  $\ell(T) = \ell_0(T) + \ell_{CP}(T)$  which includes the slow neutrino cooling [ $\ell_0(T) = \ell_C \tau^7$ ,  $\ell_C = \ell(T_C)$ ] and an extra cooling  $\ell_{CP}(T) = L_\nu^{CP}(T)/C(T)$  due to Cooper pairing of neutrons.

The Cooper pairing neutrino luminosity  $L_\nu^{CP}(T)$  has to be calculated by integration of the appropriate neutrino emissivity over the superfluid layer in the neutron star core (Gusakov et al. 2004). When the star cools, the layer becomes wider. The neutrino emissivity is a complicated function of  $T$ . Generally, the temperature dependence  $L_\nu^{CP}(T)$  is sensitive to the employed model of the star and to the model of  $T_{cn}(\rho)$ . However, as noticed by Gusakov et al. (2004), as long as  $T$  is not much lower than  $T_C$ , a superfluid layer of the core is not too wide. It is located in the vicinity of the  $T_{cn}(\rho)$  peak, and the peak can be approximated by an inverted parabolic function of radial coordinate  $r$  within the star centred at some  $r = r_C$ . In this case, the integrated neutrino luminosity  $L_\nu^{CP}(T)$  becomes a *universal* function of  $\tau$ . It was calculated by Gusakov et al. (2004) who approximated their result by an analytical expression (their eqs. 5 and 7). Their expression is cumbersome but we note that it is accurately described by a much simpler formula

$$\ell_{CP}(T) = 116 \delta \ell_C \tau^7 (1 - \tau)^2, \quad (7)$$

where  $\delta$  is a convenient dimensionless parameter that measures the efficiency of Cooper pairing neutrino emission with respect to the slow cooling level (see below). We expect that this universal formula is valid at  $0.6 \lesssim \tau \leq 1$  ( $0.6T_C \lesssim T \leq T_C$ ), although the factor 0.6 is conditional [depends on  $T_{cn}(\rho)$  model]. Notice that at  $\tau$  very close to 1, our approximation (7) is slightly inaccurate because, actually, at these  $\tau$  the function  $\ell_{CP}(\tau)$  behaves as  $(1 - \tau)^{3/2}$ . Neglecting this effect allows us to obtain analytic solution of the cooling problem at  $\tau \gtrsim 0.6$ .

Our approach tacitly assumes that neutron superfluidity does not affect the heat capacity  $C(T) \propto T$ . This is generally not true because the specific heat capacity of neutrons is affected by superfluidity (see, e.g., Yakovlev, Kaminker & Levenfish 1999). However, at the early superfluid stage, the superfluid layer within the stellar core is not too wide, so that it contributes little to the integrated heat capacity  $C(T)$ , and the assumption is justified. Using the same arguments, we also neglect the reduction of the slow component of the neutrino cooling rate,  $\ell_0(T)$ , by neutron superfluidity.

Under these assumptions, the total neutrino cooling rate at the early superfluid cooling stage ( $0.6T_C \lesssim T \leq T_C$ ) is

$$\ell(T) = \ell_C \tau^7 [1 + 116 \delta (1 - \tau)^2]. \quad (8)$$

The dependence of the neutrino cooling rate (8) on  $\tau$  for  $\delta = 0, 1, \dots, 15$  is plotted in Fig. 1. When the temperature decreases,  $\ell(T)$  rapidly decreases too as long as neutron superfluidity is absent (at  $\tau \geq 1$ ). After the superfluidity onset,  $\ell(T)$  grows up because the Cooper pairing neutrino emission starts to operate. Then, it reaches maximum and decreases again as neutron superfluidity becomes older. The maximum of the Cooper pairing neutrino cooling rate  $\ell_{CP}(T)$  takes place at  $T = T_m = 0.77 T_C$  ( $\tau_m = 0.77$ ). The maximum value of this rate is  $\ell_{CP}(T_m) = \ell_C \delta$ . Accordingly,  $\delta$  is the ratio of two neutrino cooling rates,

$$\delta = \ell_{CP}(T_m)/\ell_C, \quad (9)$$

at  $T = T_m$  and  $T = T_C$ . Note that  $\ell_{CP}(T_m)/\ell_0(T_m) = 5.8 \delta$  and  $\ell_{CP}(0.6T_C)/\ell_0(0.6T_C) = 18.56 \delta$ .

Recall that in our approach, the critical temperature  $T_{cn}(\rho(r))$  as a function of radial coordinate within the stellar core is approximated by an inverted parabola. It is determined by two parameters – the peak temperature  $T_C$  and a characteristic peak width  $\delta r_C$ . Using the results by Gusakov et al. (2004), one can show that

$$\delta = A(r_C) \delta r_C / T_C, \quad (10)$$

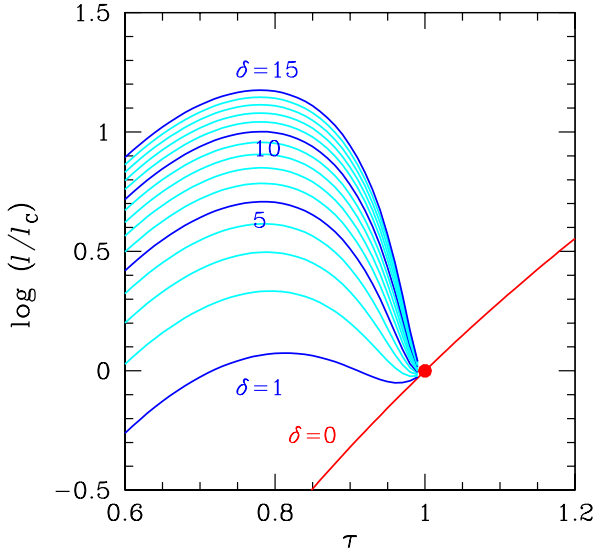


**Figure 1.** (Color on line) Normalized neutrino cooling rate  $\ell(T)/\ell_C$  versus  $\tau = T/T_C$  for  $\delta = 0, 1, \dots, 15$ . The  $\delta = 0$  curve is for a star without neutron superfluidity in the core. In other cases, neutron superfluidity of different efficiency  $\delta$  sets in at  $T = T_C$  (filled dot). This superfluidity intensifies neutrino cooling, with the maximum of the extra Cooper pairing neutrino cooling rate  $\ell_{CP}(T_m)$  at  $T = T_m = 0.77 T_C$ .

where  $A(r_C)$  is some function of  $r_C$  which is the position of the maximum  $T_{cn}$  in the core. Therefore, if we fix the neutron star model and the shape of  $T_{cn}(\rho)$  profile (i.e.  $\delta r_C$  and  $r_C$ ) but increase  $T_C$ , we would lower  $\delta \propto 1/T_C$  (i.e., lower the efficiency of the Cooper pairing neutrino cooling).

In the case of mature neutron superfluidity ( $\tau \lesssim 0.2$ , not shown in Fig. 1), the neutrino cooling rate is not described by equation (8) anymore. It can be shown (Gusakov et al. 2004; Page et al. 2004), that in this limit neutrino cooling rate behaves as  $\ell(T) \propto T^7$ . Therefore, the cooling of the star with mature superfluidity mimics the standard cooling, equation (4), but at higher cooling rate.

Now, we substitute equation (8) into equation (6). The integral is taken analytically, and we obtain

$$t = t_C [1 + 6 I_7(\tau)] \quad \text{at } t > t_C, \quad (11)$$

where  $I_7(\tau)$  belongs to a family of integrals

$$I_m(\tau) = \int_{\tau}^1 \frac{dx}{x^m [1 + 116 \delta (1-x)^2]}, \quad (12)$$

with integer  $m = 0, 1, \dots$ . These integrals are presented in Appendix A.

Now, any cooling solution can be easily calculated using equations (4) and (11) for given  $\delta$  and  $\tau \gtrsim 0.6$ . It is clear that such solutions are selfsimilar. Appropriate thermal evolution of a star is easily understood from Figs. 1–4. We have already described Fig. 1 which shows  $\ell(T)$  for  $\delta = 0, \dots, 15$ . Fig. 2 presents cooling curves (the internal temperature  $T$  versus age  $t$  in dimensionless units for the same values of  $\delta$ ). The higher  $\delta$  (the efficiency of Cooper pairing neutrino cooling), the cooler the star after superfluidity onset. Fig. 3 shows the evolution of potentially important observable

$$s = - \frac{d \ln T_s(t)}{d \ln t}, \quad (13)$$

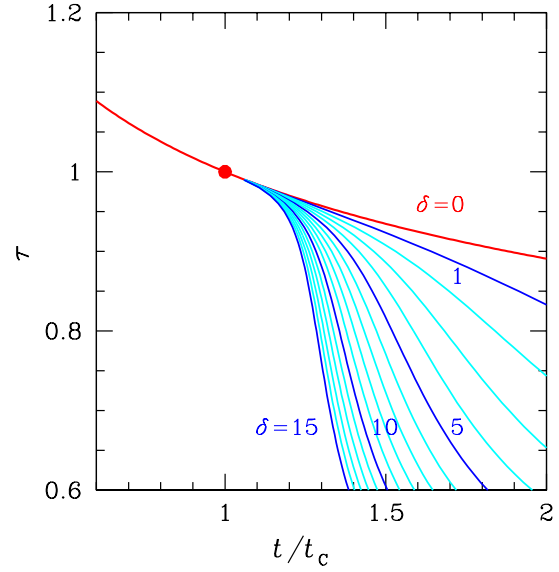


**Figure 2.** (Color on line) Normalized cooling curves  $\tau = T/T_C$  versus  $t/t_C$  for  $\delta = 0, 1, \dots, 15$  (same as in Fig. 1). After the onset of neutron superfluidity (at  $t \geq t_C$ ), the star is colder for larger  $\delta$  due to stronger Cooper pairing neutrino emission.

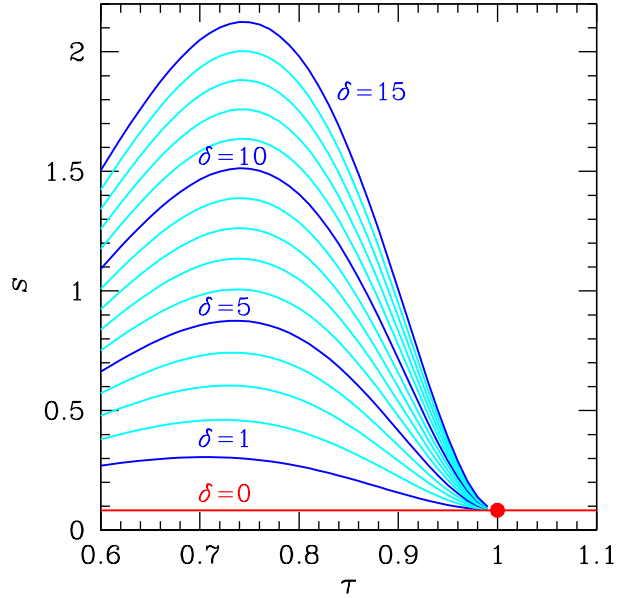


**Figure 3.** (Color on line) The slope  $s$  of the surface temperature decline versus  $\tau$  for the cooling solutions with  $\delta = 0, 1, \dots, 15$  presented in Figs. 1 and 2.

which is the (minus) logarithmic time derivative of the effective surface temperature  $T_s$  of the star [in other words, the slope of the cooling curve,  $T_s(t)$ ]. This dimensionless quantity can be measured if cooling of a neutron star is observed in real time. In order to calculate  $s$ , we need to relate the internal temperature  $T$  to  $T_s$ . It is well known (e.g., Potekhin et al. 1997) that the  $T_s$ – $T$  relation depends on the composition of the outer heat-blanketing envelope of the star (because the composition affects thermal conductivity within the envelope). However, this relation is well approximated by a power law,  $T_s \propto T^\beta$ , with  $\beta \approx 0.5$ . This makes  $s$  (but not  $T_s$

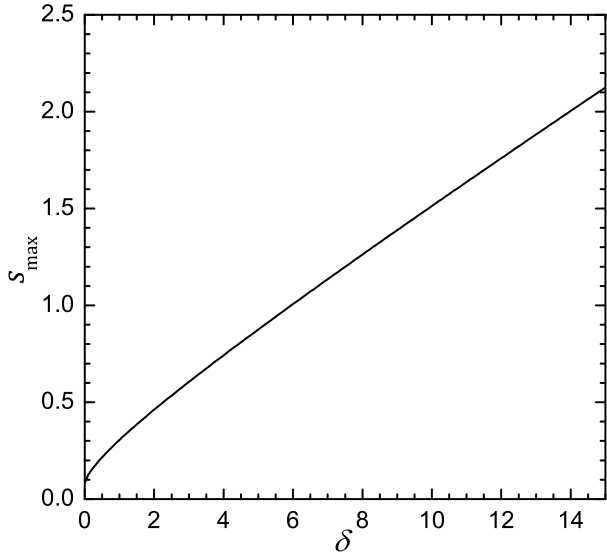


**Figure 4.** The maximum value  $s_{\max}$  of the surface temperature decline versus  $\delta$ .

itself!) *almost insensitive to the composition of the envelope*. The curves in Fig. 3 are calculated assuming  $\beta = 0.5$  from the equation

$$s = \beta \frac{d \ln T}{d \ln t} = \frac{\beta}{6\tau} \frac{t}{t_c} \frac{\ell(T)}{\ell_c}. \quad (14)$$

If neutron superfluidity is absent in the core ( $\delta = 0$  in Fig. 3) and cooling is slow, we obtain  $s = s_0 = 1/12$ . However, soon after the neutron superfluidity onset during the Cooper pairing neutrino outburst,  $s$  strongly increases, reaches maximum and then decreases again to  $s_0 = 1/12$  after superfluidity develops in the core (not shown in Fig. 3). The enhanced values of  $s(T)$  trace the neutrino cooling function  $\ell(T)$  and can serve as a sensitive indicator of a neutrino outburst in the neutron star core. Because of the peak behaviour of  $s$  as a function of  $T$  or  $t$ , there is a maximum value  $s = s_{\max}(\delta)$  for any given solution; it is reached near the maximum of the neutrino outburst. Therefore, any value of  $s$  within the range  $1/12 \leq s \leq s_{\max}$  is realized twice, before and after the maximum. The dependence of  $s_{\max}$  on  $\delta$  is plotted in Fig. 4. Equivalently, the figure presents the minimal value of  $\delta$  required to reach a given value of  $s$ .

### 3 DATA ANALYSIS USING COOLING SOLUTIONS

#### 3.1 The Cas A neutron star

Yakovlev et al. (2011) have found that the cooling of neutron stars regulated by the modified Urca process of neutrino emission is fairly independent of the equation of state (EOS) of dense stellar cores so that such stars can be used as standard cooling candles. This allowed the authors to develop a simple procedure for a model-independent analysis of the neutrino emission rates of slowly cooling stars in terms of standard candles (see also Sec. 3.3). This procedure is independent of the EOS and particular processes of slow neutrino emission in the core. Here, we extend it to the case when the early slow cooling is accelerated by the neutron superfluidity onset.

By way of illustration, consider the neutron star with the carbon atmosphere in the Cas A supernova remnant, which is currently the only isolated neutron star whose

**Table 1.** An example of Cas A neutron star model (iron heat blanket): the employed stellar mass  $M$ , radius  $R$ , age  $t_d$ , surface temperature  $T_s$ , redshifted internal temperature  $T_d$  (for the iron envelope) and the standard candle neutrino cooling rate  $\ell_{\text{SCd}}$  (for these  $M$ ,  $R$  and  $T_d$ ).

$M$ $M_\odot$	$R$ km	$t_d$ yr	$T_s$ MK	$T_d$ MK	$\ell_{\text{SCd}}$ Myr/K
1.65	11.8	330	2.0	274	0.138

cooling in real time is possibly observed (Heinke & Ho 2010). Note that after the first explanation of this effect by Page et al. (2011) and Shternin et al. (2011), several alternative explanations have been proposed (e.g. Yang, Pi & Zheng 2011, Negreiros, Schramm & Weber 2013, Sedrakian 2013, Blaschke, Grigorian & Voskresensky 2013, Bonanno et al. 2014). Moreover, the presence of real-time cooling itself has been put into question by Posselt et al. (2013) who attribute it to the *Chandra* ACIS-S detector degradation in soft channels. More observations are needed to resolve this issue.

A detailed analysis of the Cas A surface temperature decline has been done recently by Elshamouty et al. (2013) by comparing the results from all the *Chandra* detectors. They find the weighted mean of the decline rate as  $2.9\% \pm 0.5_{\text{stat}}\% \pm 1_{\text{sys}}\%$  over the 10 yr base using information from all detectors, and  $1.4\% \pm 0.6_{\text{stat}}\% \pm 1_{\text{sys}}\%$  excluding the data from the ACIS-S detector in the graded mode which can suffer from the grade migration (Elshamouty et al. 2013). With the age of the Cas A supernova remnant and its central neutron star  $t_d \approx 330$  yr, this corresponds (in our notations) to the current ( $t = t_d$ ) values  $s = s_d = 0.96 \pm 0.16_{\text{stat}} \pm 0.33_{\text{sys}}$  and  $0.46 \pm 0.20_{\text{stat}} \pm 0.33_{\text{sys}}$ , with and without ACIS-S(G) data, respectively. Recall that the standard slow cooling requires  $s = 1/12 \approx 0.08$ . The measured effective surface temperature (non-redshifted to a distant observer) is  $T_s \approx 2$  MK (Ho & Heinke 2009, see also Yakovlev et al. 2011). The spectral fits do not constrain the mass and radius of the neutron star. To be specific, we select particular  $M = 1.65 M_\odot$  and  $R = 11.8$  km, which correspond to one modification of APR EOS (Akmal, Pandharipande & Ravenhall 1998), a typical neutron star model suitable for analysing the observations of the Cas A neutron star.

If the temperature decline is due to cooling, it is inevitably small (over a limited observation history) so that in reality one obtains (detects) some mean value of  $T_s$  and the value of  $s = s_d$  (equation 13). To perform a full analysis, we need models of heat-blanketing envelope. We will employ the same carbon–iron envelope models as were used by Yakovlev et al. (2011), with  $\Delta M/M_\odot = 0, 10^{-11}$  and  $10^{-8}$  mass of carbon. The nonredshifted temperature at the bottom of heat-blanketing envelope in our example is  $T_b = 3.58, 2.59$  and  $2.05 \times 10^8$  K for the three selected amounts of carbon and the redshifted temperature of the isothermal interior is  $T_d = 2.74, 1.98$  and  $1.57 \times 10^8$  K, respectively. The envelope with carbon is more transparent to heat, making the star with this envelope colder inside than the star of the same surface temperature but with the iron envelope.

The basic parameters of the neutron star model with  $\Delta M = 0$  are collected in Table 1.

#### 3.2 Analysing data from measured values of $s_d$

First, we describe which information on neutron star physics can be extracted from the detected  $s_d$ . Since  $s_d$  is almost independent of the



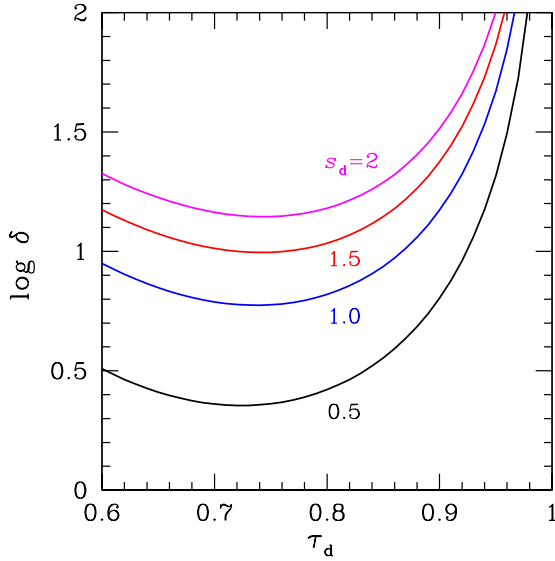


**Figure 5.** (Color on line) Four families of cooling solutions which give predetermined values  $s_d = 0.5, 1, 1.5$  and  $2$  in the present epoch  $t = t_d$ . Any solution is parametrized by  $\tau_d = T_d/T_C$ . The figure shows the parameter  $\delta$  of neutron superfluidity strength for any solution.

model of the heat-blanketing envelope, all results of this analysis also possess this property.

Let us take the theoretical expression (14) for  $s(\tau, \delta)$ , equate it to the detected  $s_d$ , and consider it as an equation to be solved. For any  $\tau_d = T_d/T_C < 1$ , we can easily solve it and find the value of  $\delta$ , which gives us a cooling solution for chosen  $s_d$  and  $\tau_d$ . In this way, we construct a family (continuum) of solutions parametrized by the values of  $\tau_d$ .

The results are illustrated in Figs. 5 and 6. In these figures, we display four families of such solutions which correspond to  $s_d = 0.5, 1, 1.5$  and  $2$ . Figs. 5 and Fig. 6 show, respectively, the values of  $\delta$  and  $t_c/t_d$  versus  $\tau_d$ . In addition, the right vertical scale in Fig. 6 presents the time  $t_c$  of neutron superfluidity onset in the Cas A neutron star. For higher  $s_d$ , one naturally needs stronger neutrino cooling due to Cooper pairing neutrino emission (larger  $\delta$ ). For a given  $s_d$ , the lowest  $\delta$  corresponds to the vicinity of  $\tau_d = T_d/T_C \approx 0.77$  (to the peak of Cooper pairing neutrino outburst in the present epoch). The limit of  $\tau_d \rightarrow 1$  is equivalent to  $T_C \rightarrow T_d$  [the epoch  $t_c$  of neutron superfluidity onset approaches the present (detection) epoch  $t_d$ ].

Let us emphasize that families of cooling solutions for fixed  $s_d$  are really *selfsimilar and universal*. They are not only *independent of the model for the heat-blanketing envelope* but *independent also of the neutron star model (mass, radius, the EOS) as well as of absolute value of the surface temperature  $T_s$* . All these dependences are encapsulated in the values of introduced dimensionless parameters. If, by any chance, one of them is known (for instance,  $\delta$ , from a given model of neutron superfluidity), then one can use this known value and find  $\tau_d$ . In this case, one would select a unique solution of the cooling problem (or a pair of them) from the entire family. Otherwise, one should face the family of solutions with different  $\tau_d$ .

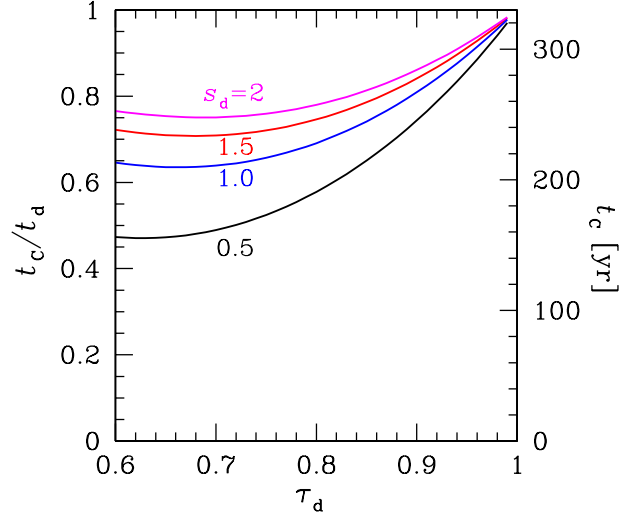


**Figure 6.** (Color on line) The same four families of cooling solutions for  $s_d = 2, 1.5, 1$  and  $0.5$  as in Fig. 5. The figure presents  $t_c/t_d$  (left vertical scale) for any  $\tau_d = T_d/T_C$ . For illustration, the right vertical scale gives  $t_c$  for the Cas A neutron star.

### 3.3 Solutions with particular $\tau_d$

Here, we describe which additional information can be inferred from observations provided particular  $\tau_d$  is selected. Let us take the corresponding cooling solution from the family described in Section 3.2 (with the iron heat-blanketing envelope as an example). Using the values of  $\tau_d$  and  $T_d$ , we immediately find the maximum critical temperature of neutron superfluidity,  $T_C$ . Using equation (11) as well as specific values of  $\tau_d$  and  $\delta$ , one can determine  $t_d/t_c$  and obtain the time  $t_c$  of neutron superfluidity onset.

According to Yakovlev et al. (2011), it is convenient to describe the neutrino emission level via the ratio

$$f_\ell = \ell(T)/\ell_{SC}(T) \quad (15)$$

of the neutrino cooling rate  $\ell(T)$  of our star to the neutrino cooling rate  $\ell_{SC}(T)$  of the standard candle (the star of the same  $M$  and  $R$  which cools slowly via modified Urca process) at the same internal temperature. At  $t < t_c$ , the cooling is slow and the factor  $f_\ell = f_{\ell 0}$  is just a number (independent of  $T$ ) which reflects the neutrino cooling level prior to superfluidity onset. This level can be determined from  $t_c$  and  $T_C$  as

$$f_{\ell 0} = [T_{SC}(t_c)/T_C]^6, \quad (16)$$

where  $T_{SC}(t)$  is given by equation 14 of Yakovlev et al. (2011).

Now, one has everything at hand to fully reconstruct the cooling history of the star in absolute and dimensionless variables for any cooling solution of the family. Any solution is characterized by the parameters  $f_{\ell 0}$ ,  $\delta$  and  $T_C$  which determine the efficiency of neutrino cooling. The value of  $f_{\ell 0}$  contains all the information on the neutrino cooling in the early epoch when neutron superfluidity in the core is absent. The values of  $T_C$  and  $\delta$  describe neutron superfluidity and the neutrino cooling rate after the neutron superfluidity onset. This analysis is independent of a specific model of neutron

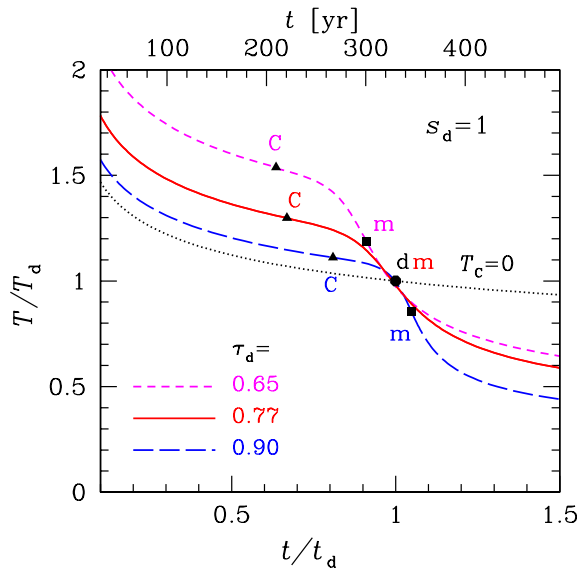


**Figure 7.** (Color on line) Evolution of internal temperature  $T/T_d$  versus  $t/t_d$  for in the  $1.65 M_\odot$  neutron star in Cas A with iron heat-blanketing envelope, nonredshifted surface temperature  $T_{sd} = 2$  MK ( $T_d = 274$  MK) and  $s_d = 1$  at  $t = t_d = 330$  yr for the three values  $\tau_d = T_d/T_C = 0.65, 0.77$  and  $0.9$  (short-dashed, solid and long-dashed lines, respectively). Moments of time ‘C’ when neutron superfluidity sets in are denoted by triangles. Moments ‘m’ of maximum Cooper pairing neutrino emission rate ( $\tau = 0.77$ ) are labelled by squares, while ‘d’ refers to the moment of observation. The dotted line shows the evolution of the star without neutron superfluidity. The upper horizontal scale gives real time  $t$ . See text for details.

**Table 2.** Three cooling solutions for the Cas A neutron star model with iron heat blanket and  $s_d = 1$ . See text for details.

$\tau_d$	$\delta$	$\Delta t_C^{(a)}$ yr	$T_C$ MK	$\Delta t_m^{(b)}$ yr	$s_{max}$
0.65	7.046	120	422	29	1.05
0.77	6.111	109	356	0	1.00
0.90	14.88	63	304	-16	2.23

<sup>(a)</sup>  $\Delta t_C = t_d - t_C$

<sup>(b)</sup>  $\Delta t_m = t_d - t_m$

star (with nucleon core). Specific physical models which agree with the inferred results can be analysed at a later stage.

For illustration, consider three cooling solutions for  $s_d = 1$  at  $\tau_d = 0.65, 0.77$  and  $0.9$ . Some parameters of these solutions are listed in Table 2, where  $\Delta t_C = t_d - t_C$  and  $\Delta t_m = t_d - t_m$  (where  $t_m$  is the time corresponding to  $\tau = \tau_m = 0.77$ ).

Fig. 7 shows the internal thermal evolution ( $T/T_d$  versus  $t/t_d$  or  $t$ , lower or upper horizontal scales, respectively) of the Cas A neutron star assuming the iron heat-blanketing envelope ( $T_d = 2.74 \times 10^8$  K). It is additionally assumed that at  $t = t_d$  the surface temperature decline is  $s_d = 1$ . The surface temperature behaves approximately as  $T_s(t) \approx T_s(t_d)(T(t)/T_d)^{0.5}$ . We show the three cooling curves parametrized by  $\tau_d = 0.65, 0.77$  and  $0.9$  (the short-dashed, solid and long-dashed curves, respectively). These are three possible cooling scenarios (among continuum of others), which give the same temperature and temperature decline of the star in the observation epoch (filled point ‘d’). They differ by  $\tau_d$ , that is by the maximum critical temperature  $T_C$  for neutron superfluidity in the core

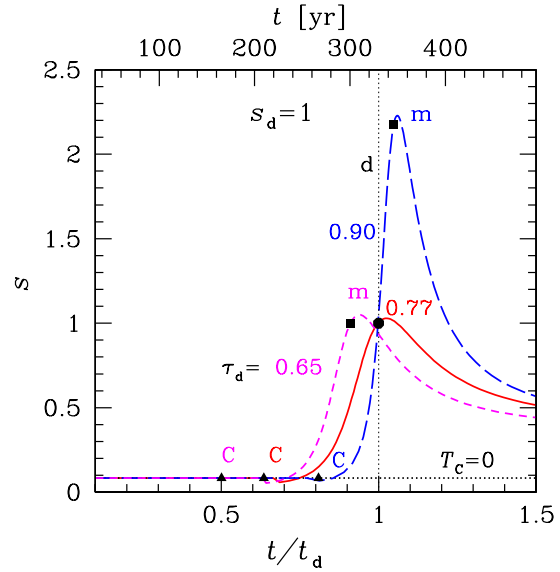


**Figure 8.** (Color on line) Evolution of surface temperature decline  $s$ , equation (14), of the Cas A neutron star calculated for the same three cooling scenarios ( $\tau_d = 0.65, 0.77$  and  $0.9$ ) as in Fig. 7. The vertical dotted line shows the present-time epoch. See text for details.

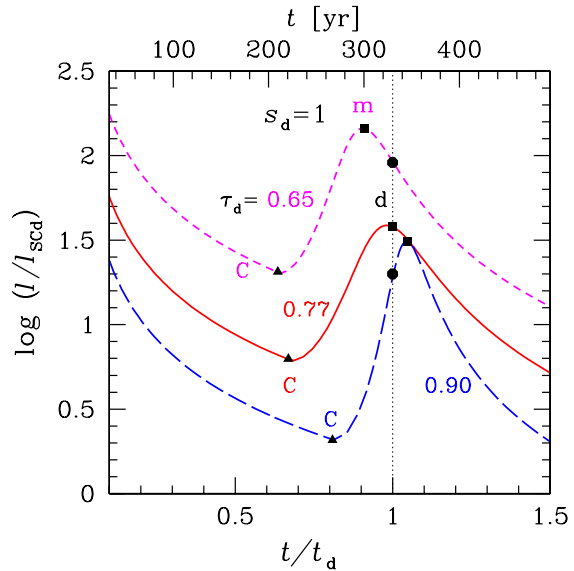


**Figure 9.** (Color on line) Evolution of neutrino cooling rate  $\ell$  (in units of  $\ell_{scA}$  of standard neutrino candle at  $t = t_d$ , Table 2) of the Cas A neutron star for the same three cooling scenarios as in Figs. 7 and 8. The vertical dotted line shows the present-time epoch. See text for details.

(Table 2). The moments of time ‘C’, when neutron superfluidity appears in the core (120, 109 and 63 yr ago, for  $\tau_d = 0.65, 77$  and  $0.9$ , respectively), are marked by triangles on the cooling curves. The higher  $T_C$ , the earlier it should appear. By squares (points ‘m’), we mark the moments of maximum Cooper pairing neutrino emission rate ( $\tau = 0.77$ , approximately, the maximum of neutrino outburst). In case  $\tau_d = 0.65$ , this maximum is reached 29 yr before the observation epoch, while in case  $\tau_d = 0.9$ , it occurs 16 yr after the

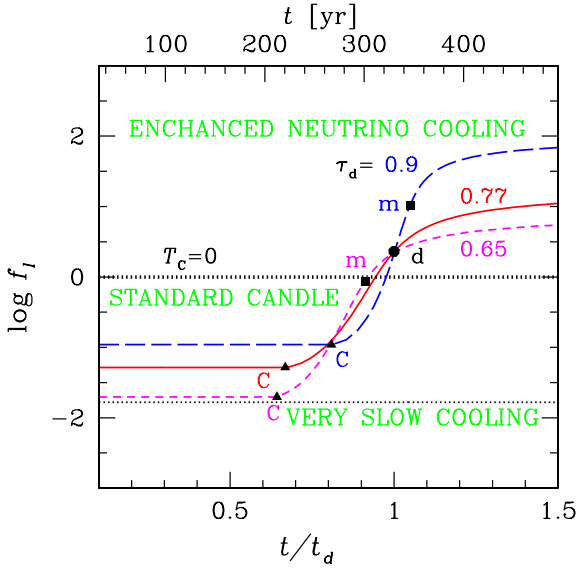
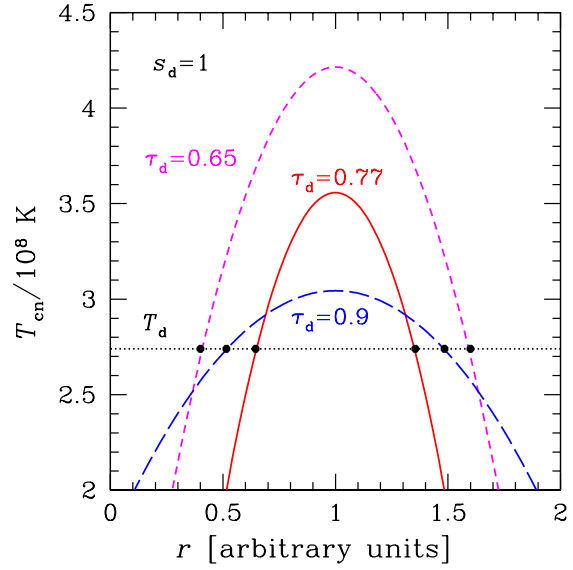


**Figure 10.** (Color on line) Evolution of neutrino cooling rate  $f_\ell$  (in standard candles) of the Cas A neutron star for the same three cooling scenarios ( $\tau_d=0.65$ ,  $0.77$  and  $0.9$ ) as in Figs. 7–9. The horizontal thicker dotted line  $f_\ell = 1$  refers to the standard neutrino candle; the thinner dotted line  $f_\ell = 1/60$  is the estimated lowest theoretical rate. See text for details.

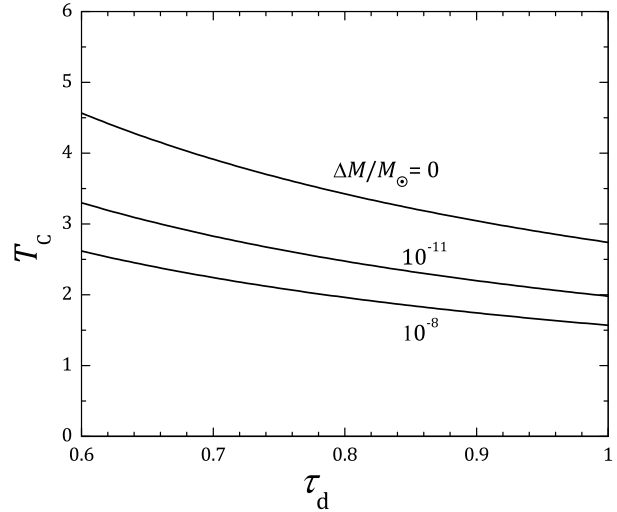
observation epoch. If  $\tau_d = 0.77$ , it occurs just now. By the dotted line, we plot the cooling curve calculated neglecting neutron superfluidity and slightly adjusting the modified Urca neutrino emission level to give the same current temperature  $T_d$  of the star, as other curves. This cooling gives too low  $s = 1/12$  and would be not detectable in real time for the Cas A neutron star.

Fig. 8 presents the evolution of the surface temperature decline  $s$  for the same three cooling scenarios of the Cas A neutron star as in Fig. 7, and for the standard neutrino candle without neutron superfluidity. The notations are the same as in Fig. 7. In the scenario with  $\tau_d = 0.65$ , the maximum  $s_{\max} \approx 1.05$  is reached prior to the detection epoch (about 20 yr ago), so that  $s(t)$  decreases with time during the detection epoch. This scenario is qualitatively consistent with those suggested by Page et al. (2011) and Shternin et al. (2011). In the scenario with  $\tau_d = 0.9$ ,  $s(t)$  has not yet reached its maximum at the present epoch. Accordingly,  $s(t)$  sharply increases with  $t$  and will reach maximum  $s_{\max} \approx 2.23$  in about 20 yr from now. At  $\tau_d = 0.77$ , the maximum value  $s_{\max} \approx 1$  is reached just now. Therefore,  $s(t)$  should decrease in time but in the next 20 years the decrease should be very slow. Let us remark that the maxima of  $s(t)$  are close to but do not coincide with the maxima of  $\ell_{\text{CP}}(t)$ . The stronger the Cooper pairing neutrino emission, the better the coincidence.

Fig. 9 displays the evolution of the neutrino cooling rate  $\ell$  (in the units of the rate  $\ell_{\text{SCd}} = \ell_{\text{SC}}(t_d) = 0.138 \text{ MK yr}^{-1}$  for the standard candle in the present epoch, see Table 1) for the same three scenarios as in Figs. 7 and 8. Prior to the neutron superfluidity onset, we have  $\ell(T) \propto T^7$ . With increasing  $\tau_d$ , we need lower  $\ell(t)$ . After superfluidity onset, the rate is enhanced by the neutrino outburst with the maximum before the detection epoch (at  $\tau_d = 0.65$ ), just now ( $\tau_d = 1$ ) or afterwards ( $\tau_d = 0.9$ ). Again, the maxima of  $\ell(t)$  do not exactly coincide with the maxima of  $\ell_{\text{CP}}(t)$  (with points ‘m’) but the coincidence becomes better for stronger Cooper pairing neutrino emission.



**Figure 11.** (Color on line) Examples of the three neutron superfluidity profiles  $T_{\text{cn}}(r)$  over the neutron star core which produce the cooling solutions for  $\tau_d=0.65$  (short-dashed line),  $0.77$  (solid line) and  $0.9$  (long dashes), respectively. The radial coordinate  $r$  is in arbitrary units. The dotted horizontal line is the core temperature in the present epoch. Filled dots show the boundaries of superfluid layers in the three cases.



**Figure 12.** Maximum (redshifted) critical temperature for neutron superfluidity  $T_C$  (which is independent of  $s_d$ ) versus  $\tau_d$  in the  $1.65 M_\odot$  model of the Cas A neutron star at three values of  $\Delta M/M_\odot$  shown near the lines ( $\Delta M$  being the carbon mass in the heat-blanketing envelope; see text for details).

Fig. 10 demonstrates the evolution of neutrino cooling rate  $f_\ell(t)$ , expressed in standard neutrino candles according to equation (15), for the same three cooling scenarios ( $\tau_d=0.65$ ,  $0.77$  and  $0.9$ ) as in Figs. 7–9. Note that  $f_\ell = 1$  ( $\log f_\ell = 0$ ) refers to the standard neutrino candle,  $\log f_\ell \gtrsim 2$  to rather enhanced neutrino cooling and  $\log f_\ell \lesssim -2$  to unrealistically slow cooling. We see that prior to the neutron superfluidity onset (before triangles),  $f_\ell = f_{\ell 0}$  is constant and rather low. This agrees with numerical simulations of the Cas A neutron star cooling by Page et al. (2011) and Shternin et al.

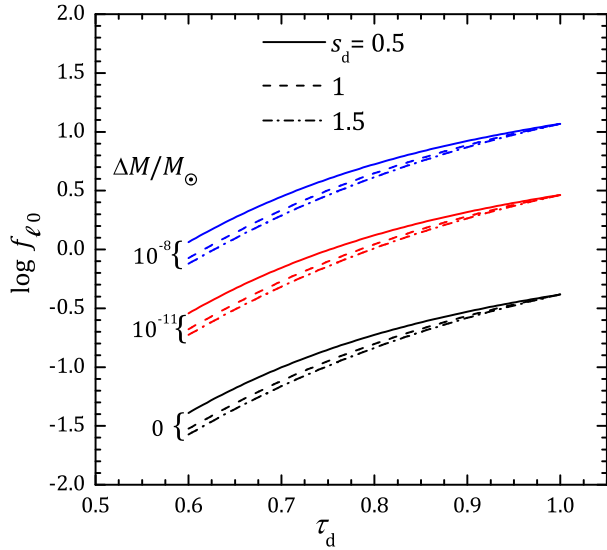


**Figure 13.** (Color on line) Neutrino cooling rate  $f_{\ell 0}$  (in standard candles) for the Cas A neutron star model before the neutron superfluidity onset for three families of cooling solutions ( $s_d = 0.5, 1, 1.5$ ) versus  $\tau_d$  at the three values of  $\Delta M/M_\odot$  (the same as in Fig. 12) indicated in the plot.

(2011). With increasing  $\tau_d$  (or, equivalently, decreasing  $T_C$ ), one needs higher  $f_{\ell 0}$ . At very low  $\tau_d$ , one would need too slow neutrino cooling rate before the neutron superfluidity onset. For instance,  $f_{\ell 0}$  cannot be  $\lesssim 1/60$  (thinner horizontal dotted line in Fig. 10) because proton superfluidity cannot produce too strong reduction of the slow cooling rate with respect to the modified Urca rate (there are always processes, such as neutron–neutron or electron–electron neutrino bremsstrahlung, which do not involve protons; they are almost insensitive to the presence of proton superfluidity). Such cases are unrealistic and should be disregarded.

After the neutron superfluidity is switched on,  $f_{\ell}(t)$  in Fig. 10 grows up (during the neutrino outburst) and then has the tendency to saturate at much higher level than at the initial cooling stage. This saturation reflects the fact that the neutrino emission due to Cooper pairing of neutrons in a developed neutron superfluidity has the same temperature dependence as the standard candle ( $\ell \propto \tau^7$ ) but can be substantially enhanced with respect to the standard candle (Page et al. 2004, Gusakov et al. 2004). The higher  $\tau_d$ , the larger enhancement. Very large enhancements  $f_{\ell} \gtrsim 10^2$  are unrealistic and should be disregarded.

Fig. 11 demonstrates possible  $T_{cn}(r)$  profiles as a function of radial coordinate  $r$  within the neutron star core. These profiles can realize cooling solutions with  $\tau_d = 0.65, 0.77$  and  $0.90$  (short-dashed, solid and long-dashed lines, respectively). The profiles are approximated by inverted parabolas whose maxima are at the same position  $r_C$  in the star. The maximum heights  $T_C$  and the parameters  $\delta$  have already been determined (Table 2). The characteristic widths  $\Delta r_C$  of the parabolas are found from equation (10) [up to a joint normalization factor determined by the coefficient  $A(r_C)$ ; to avoid cumbersome calculation of  $A(r_C)$ , we plot radial coordinates in arbitrary units]. The horizontal dotted line shows the present-day temperature  $T_d$  in the core. Neutron superfluidity exists at those  $r$  at which  $T_{cn}(r) \geq T_d$ . The boundaries of superfluid layers are marked by dots. For the solution with  $\tau_d = 0.65$ , the  $T_{cn}(r)$  profile is sufficiently high. For  $\tau_d = 0.77$ , it is smaller, while for  $\tau_d$ , it is even smaller but wider. The increased width is needed to obtain large  $\delta = 14.88$ . Naturally, Fig. 11 presents only some examples of  $T_{cn}(r)$

profiles. The same cooling solutions can be realized with other profiles [different values of  $r_C$  and  $A(r_C)$  in equation (10)] which result in the same  $\delta$ .

### 3.4 Effects of carbon heat-blanketing envelope and different $s_d$

So far, we have analysed cooling models of the Cas A neutron star only at  $s_d = 1$  and with standard heat-blanketing envelopes made of iron. Let us outline the effects of possible carbon heat blankets and different present-day slopes  $s_d$  of the cooling curves.

Fig. 12 presents the maximum critical temperature  $T_C$  for neutron superfluidity in the core of the  $1.65 M_\odot$  neutron star (the same as considered throughout this paper) for different cooling solutions parametrized by  $\tau_d$ . They are apparently determined by  $T_d$  being independent of  $s_d$ . The upper line corresponds to the iron heat blanket while two lower lines refer to the heat blankets containing  $\Delta M = 10^{-11}$  and  $10^{-8} M_\odot$  of carbon, respectively. The presence of carbon makes the heat-blanketing envelope more heat transparent and reduces the critical temperature  $T_C$  required to satisfy cooling solutions. The reduction is seen to be quite substantial.

Fig. 13 shows logarithm of the neutrino cooling rate  $f_{\ell 0}$  (in standard candles) prior to the onset of neutron superfluidity for the cooling solutions as a function of  $\tau_d$ . We show three groups of curves, again for  $\Delta M/M_\odot = 0, 10^{-11}$  and  $10^{-8}$  (from top to bottom). For each amount of carbon  $\Delta M$ , we present the solutions for  $s_d = 0.5$  (solid lines),  $1$  (dashed lines) and  $1.5$  (dot-dashed lines). Higher amount of carbon leads to lower  $T_d$  and the solutions require larger  $f_{\ell 0}$ ; for larger  $s_d$ , they require lower  $f_{\ell 0}$ . It is seen that  $f_{\ell 0}$  is rather insensitive to  $s_d$  in the given  $s_d$  interval.

One can see that for the cases of iron envelope and envelope with  $10^{-11} M_\odot$  of carbon, the slow cooling rate prior to the neutron superfluidity onset should be lower than for the standard candle. This lowering can be provided by strong proton superfluidity in the neutron star core. With the growth of  $\tau_d$ , the required lowering is smaller. Taking highest amount of carbon ( $\Delta M = 10^{-8} M_\odot$ ), one will need the standard cooling rate, or even enhanced cooling at  $t < t_C$ .

These solutions can be constrained further by taking into account natural physical restrictions. Recall that  $f_{\ell 0}$  should be  $\gtrsim 1/60$ . For the iron envelope model, this invalidates cooling solutions with rather small  $\tau_d$  and large  $s_d$ . On the other hand,  $f_{\ell 0}$  cannot be arbitrarily large as this would require unphysically strong neutrino outburst after superfluidity onset to reach the same  $s_d$  (the same  $\delta$ ) at the present epoch.

According to equation (9),  $\delta$  is inversely proportional to the value  $\ell_C$  which determines the neutrino emission rate prior to neutron superfluidity onset. In addition, as seen from (10),  $\delta \propto T_C^{-1}$ . Therefore, it is instructive to introduce the new parameter

$$T_{C0} = f_{\ell 0} T_C \delta \quad (17)$$

instead of  $\delta$ . Its dimension is temperature but it characterizes the volume of the region occupied by neutron superfluidity in the star. Because of the factor  $f_{\ell 0}$  in equation (17) the dependence of  $T_{C0}$  on the neutrino emission level prior the neutron superfluidity onset is eliminated. If we fix  $r_C$  but increase  $\delta r_C$ , we would amplify  $T_{C0} \propto \delta r_C$  (see equation (10)). In Fig. 14, we plot  $T_{C0}$  versus  $\tau_d$  for the selected values of  $s_d$  and  $\Delta M$ . This figure demonstrates the dependence of the peak's width  $\delta r_C$  on its height  $T_C$  for selected families of cooling solutions characterized by  $s_d$  and  $\tau_d$ . For a given  $s_d$ , higher  $\tau_d$  would require wider  $T_{cn}(r)$  peaks (larger  $\delta r_C$ ). Equally, at a fixed  $\tau_d$ , higher  $s_d$  require larger  $\delta r_C$ . Naturally,  $\delta r_C$  is limited



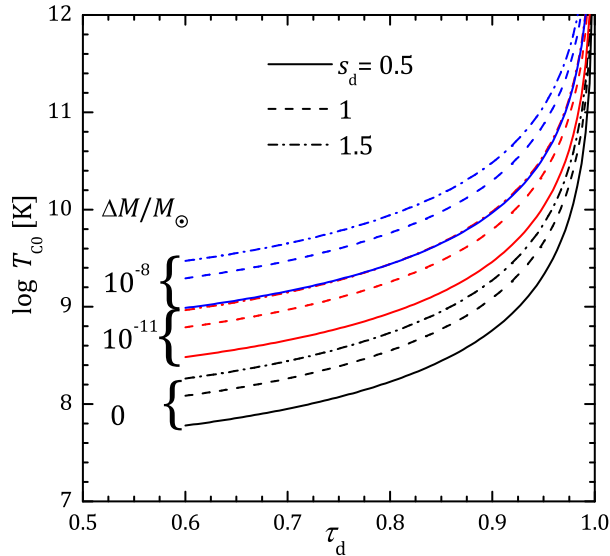


**Figure 14.** (Color on line) Parameter  $T_{C0}$  versus  $\tau_d$  for three families of cooling solutions ( $s_d = 0.5, 1, 1.5$ ) and three values of  $\Delta M/M_\odot$  (as in Fig. 13).

by the size of the neutron star core so that  $T_{C0}$  cannot be arbitrarily large.

According to cooling simulations, realistic models of neutron superfluidity correspond to  $T_{C0} \lesssim 3 \times 10^8$  K. As an example, consider the Cas A neutron star at  $s_d = 1$ . From Fig. 14, we find  $\tau_d \lesssim 0.75$  for the iron heat blanket. Then, Fig. 13 implies  $f_{i0} \lesssim 0.1$ . Lower values of  $\tau_d$  require lower  $T_{C0}$ , i.e. smaller volume occupied by neutron superfluidity or weaker efficiency of the Cooper pairing neutrino emission. However, the price to pay is that the  $f_{i0}$  should also be lower. Taking into account that  $f_{i0}$  cannot be too small and  $\tau_d \gtrsim 0.6$ , we obtain an approximate constraint  $3.5 \times 10^8 \lesssim T_C \lesssim 4.5 \times 10^8$  K. This in turn means that real (non-redshifted) maximum critical temperature of neutrons lies in the range  $\sim (5 - 8) \times 10^8$  K depending on the position  $r_C$  of the maximum critical temperature  $T_{cn}$  inside the core for our  $1.65 M_\odot$  neutron star model. The restriction of low  $T_{C0}$  forbids significant amount of carbon in the envelope in our example. According to Figs. 13 and 14, the values  $\Delta M \gtrsim 10^{-11} M_\odot$  are inconsistent with the observations if  $s_d = 1$ . If  $s_d = 0.5$ , then  $\Delta M \sim 10^{-11} M_\odot$  is allowed but with fine tuning of the parameters to obey  $\tau_d \lesssim 0.6$ . For this solution we need  $f_{i0} < 0.3$  (Fig. 13), i.e. we also need (not very strong) proton superfluidity in the core. Note that numerical cooling solutions with  $\tau_d < 0.6$  follow the general trend of Figs. 13–14. However, strictly speaking, our simple analytical formalism is inapplicable at such low  $\tau_d$ . On the other hand, in case  $s_d = 1$  neutron superfluidity should be inevitably rather strong, so that  $T_{C0} > 10^8$  K.

Note that the limit  $T_{C0} \lesssim 3 \times 10^8$  K was estimated using the same model for treating the collective effects on the efficiency of Cooper pairing neutrino emission as adopted by Page et al. (2009, 2011) and Shternin et al. (2011) (their reduction factor  $q = 0.76$  of the neutrino emissivity by the collective effects). In this model, the emission in the vector channel is fully suppressed by the collective effects, while the emission in the axial vector channel remains unchanged. According to Leinson (2010), collective effects may actually lower the neutrino emission efficiency four times more ( $q = 0.19$  in Shternin et al. 2011). The latter case corresponds to the restriction  $T_{C0} \lesssim 0.75 \times 10^8$  K. According to Fig. 13, it is im-

possible to get  $s_d = 1$  with such  $T_{C0}$ . If, however, the cooling of the Cas A neutron star is slower, with  $s_d \sim 0.5$ , then we again can explain the observations, provided  $\tau_d < 0.66$ , even for such a low efficiency of Cooper pairing neutrino emission. In this case, we need strong proton superfluidity (low  $f_{i0}$ ), and a small amount of carbon in the heat-blanketing envelope.

Of course, the described procedure of data analysis is idealized. All observables ( $M$ ,  $R$ ,  $T_s$ ,  $t_d$ ) are always determined with some uncertainties. This biases the analysis of the data and introduces uncertainties into final results.

We have compared some analytic cooling solutions with those obtained with our cooling code (Gnedin, Yakovlev & Potekhin 2001) and found out impressive agreement. Notice, however, that, according to the exact solutions, the appearance of neutron superfluidity and the associated neutrino outburst slightly violate isothermality of the core (e.g., Shternin et al. 2011) but this violation has no noticeable effect on the cooling curves.

## 4 CONCLUSIONS

We have analysed the cooling of a neutron star with the thermally relaxed nucleon core at the neutrino cooling stage ( $10^2 \lesssim t \lesssim 10^5$  yr). For simplicity, we have considered neutron star models where direct Urca process does not operate. We have assumed further that the star has strong proton superfluidity in the core, which appears at the early cooling stage, and moderately strong (triplet-state) neutron superfluidity which appears later, when the internal temperature of the star,  $T$ , falls below  $T_C$ , the maximum critical temperature for neutron superfluidity over the stellar core (equation (1)). Therefore, the star cools slowly before the neutron superfluidity onset ( $T > T_C$ ,  $t < t_C$ ) but its cooling is accelerated later by the appearance of neutron superfluidity and associated outburst of the neutrino emission due to Cooper pairing of neutrons.

Our analysis is based on the results by Gusakov et al. (2004) according to which at  $T$  not much lower than  $T_C$ , the neutrino luminosity  $L_\nu^{\text{CP}}(T)$  due to Cooper pairing of neutrons has a universal form. We show that at these temperatures,  $0.6 T_C \lesssim T < T_C$ , the neutrino cooling rate  $\ell(T) = L_\nu(T)/C(T)$  is approximated by the simple expression (8), and the cooling problem is solved in a closed analytic self-similar forms (4) and (6). Any solution can be parametrized by the values of  $\tau_d = T_d/T_C$  and  $s_d$  (the slope of the cooling curve in the present epoch,  $t = t_d$ ). Formally, for a fixed  $s_d$ , there exists a continuum of solutions which differ by the values of  $\tau_d$ . We have analysed the properties of these solutions and the methods to select physically sound ones. In the essence, the solutions differ by the profiles  $T_{cn}(\rho)$  and  $T_{cp}(\rho)$  of critical temperatures for neutron and proton superfluidity in the neutron star core. However, our analytic approach allows one to describe the effects of these superfluidities on the neutron star cooling by two dimensionless parameters,  $f_{i0}$  [equation (16), reflects the neutrino cooling rate prior to neutron superfluidity onset, regulated by proton superfluidity], and  $\delta$  [equation (9), characterizes the efficiency of neutrino outburst due to neutron superfluidity]. We have described how to infer allowable values of these parameters from observations of neutron stars whose cooling in real time is observed, using the Cas A neutron star as the only example known today.

The advantage of our method is that it gives all possible solutions of the cooling problem. One can analyse them and determine all the values of the parameters (particularly,  $f_{i0}$  and  $\delta$ ); whereas physical models of superfluidity [ $T_{cn}(\rho)$  and  $T_{cp}(\rho)$ ] can be investigated at the later stage. In this way, we have extended the model

independent method of data analysis of cooling neutron stars suggested by Yakovlev et al. (2011). The latter authors developed this method for slowly cooling neutron stars. We have included a more complicated case of neutron superfluidity onset.

The analytic solution can be used to interpret observations of cooling neutron stars in real time (when one can measure the surface temperature of the star  $T_s$  and the rate  $s_d$  of its decline). We have described the procedure (Section 3) how to interpret such observations, to reconstruct the cooling history of the neutron star and predict its future cooling behaviour (for future observational tests). We have presented examples of such interpretations for the Cas A neutron star. In particular, one needs to suppress the neutrino emission prior to the neutron superfluidity onset below the modified Urca level even if the rapid cooling in real time at the present epoch is twice slower than estimated by Heinke & Ho (2010). Moreover, we have shown that large amount of carbon in the heat-blanketing envelope is inconsistent with observations of this object.

Because the observations of this star are still a subject of debates (Section 3.1), one should be ready to analyse the data under different assumptions. The presented formalism seems perfect for this purpose. If the data by Elshamouty et al. (2013) are confirmed in future observations, the assumption by Page et al. (2011) and Shternin et al. (2011) that the cooling is regulated by the effects of neutron superfluidity would remain realistic and attractive explanation. The main indicator in favour for this conclusion would be the observed value of the surface temperature decline,  $s_d$ ; it has to be noticeably larger than 0.1. If the data disfavour such large  $s_d$  (Posselt et al. 2013), the theory can help imposing some constraints on the properties of superfluidity in the stellar core.

## ACKNOWLEDGEMENTS

This work was partly supported by RFBR (grants 14-02-00868-a and 13-02-12017-ofi-M) and RF Presidential Programme NSh-294.2014.2.

## APPENDIX A: CALCULATION OF COOLING INTEGRALS

We deal with the family of integrals

$$I_m(\tau) = \int_{\tau}^1 \frac{dx}{x^m [1 + \alpha(1-x)^2]}, \quad (\text{A1})$$

with integer  $m = 0, 1, \dots$  and  $\alpha = 116\delta$ . These integrals satisfy useful recurrent relations

$$(1 + \alpha) I_m(\tau) = J_m(\tau) + 2\alpha I_{m-1}(\tau) - \alpha I_{m-2}(\tau) \quad (\text{A2})$$

with

$$\begin{aligned} J_m(\tau) &= \int_{\tau}^1 \frac{dx}{x^m} = \frac{1}{m-1} \left( \frac{1}{\tau^m} - 1 \right), \\ I_1(\tau) &= \frac{1}{2(1+\alpha)} \ln \left( \frac{1 + \alpha(1-\tau)^2}{\tau^2} \right) + \frac{\alpha}{1+\alpha} I_0(\tau), \\ I_0(\tau) &= \frac{1}{\sqrt{\alpha}} \arctan \left( \sqrt{\alpha}(1-\tau) \right). \end{aligned}$$

These relations allow one to calculate (A1) at any  $m$ .

## REFERENCES

- Akmal A., Pandharipande V. R., Ravenhall D. G., 1998, *Phys. Rev. C*, 58, 1804
- Blaschke D., Grigorian H., Voskresensky D. N., 2013, *Phys. Rev. C*, 88, 065805
- Bonanno A., Baldo M., Burgio G. F., Urpin V., 2014, *A&A*, 561, L5
- Elshamouty K. G., Heinke C. O., Sivakoff G. R., Ho W. C. G., Shternin P. S., Yakovlev D. G., Patnaude D. J., David L., 2013, *ApJ*, 777, 22
- Gnedin O. Y., Yakovlev D. G., Potekhin A. Y., 2001, *MNRAS*, 324, 725
- Gusakov M. E., Kaminker A. D., Yakovlev D. G., Gnedin O. Y., 2004, *A&A*, 423, 1063
- Heinke C. O., Ho W. C. G., 2010, *ApJ*, 719, L167
- Ho W. C. G., Heinke C. O., 2009, *Nature*, 462, 71
- Leinson L. B., 2010, *Phys. Rev. C*, 81, 025501
- Lombardo U., Schulze H.-J., 2001, in D. Blaschke, N. K. Glendenning, A. Sedrakian, eds, *Lecture Notes in Physics*, Vol. 578, *Physics of Neutron Star Interior*, Springer Verlag, Berlin, p. 30
- Negreiros R., Schramm S., Weber F., 2013, *Phys. Lett. B*, 718, 1176
- Page D., Lattimer J. M., Prakash M., Steiner A. W., 2004, *ApJ*, 155, 623
- Page D., Lattimer J. M., Prakash M., Steiner A. W., 2009, *ApJ*, 707, 1131
- Page D., Prakash M., Lattimer J. M., Steiner A. W., 2011, *PRL*, 106, 081101
- Posselt B., Pavlov G. G., Suleimanov V., Kargaltsev O., 2013, *ApJ*, 779, 186
- Potekhin A. Y., Chabrier G., Yakovlev D. G., 1997, *A&A*, 323, 415
- Sedrakian A., 2013, *A&A*, 555, L10
- %
- Shternin P. S., Yakovlev D. G., Heinke C. O., Ho W. C. G., Patnaude D. J., 2011, *MNRAS*, 412, L108
- Yakovlev D. G., Pethick C. J., 2004, *ARA&A*, 42, 169
- Yakovlev D. G., Kaminker A. D., Levenfish K. P., 1999, *A&A*, 343, 650
- Yakovlev D. G., Ho W. C. G., Shternin P. S., Heinke C. O., Potekhin A. Y., 2011, *MNRAS*, 411, 1977
- Yang S.-H., Pi C.-M., Zheng X.-P., 2011, *ApJL*, 735, L29